

1 **Title:** Human Heart Failure Alters Mitochondria and Fiber 3D Structure Triggering Metabolic  
2 Shifts

3 **Authors:**

4 Zer Vue<sup>\*1</sup>, Peter T. Ajayi<sup>\*2</sup>, Kit Neikirk<sup>1</sup>, Alexandria C. Murphy<sup>3</sup>, Praveena Prasad<sup>3</sup>, Brenita C.  
5 Jenkins<sup>3</sup>, Larry Vang<sup>1</sup>, Edgar Garza-Lopez<sup>4</sup>, Margaret Mungai<sup>1</sup>, Andrea G. Marshall<sup>1</sup>, Heather K.  
6 Beasley<sup>1</sup>, Mason Killion<sup>1</sup>, Remi Parker<sup>1</sup>, Josephs Anukodem<sup>1</sup>, Kory Lavine<sup>5</sup>, Olujimi Ajijola<sup>6</sup>,  
7 Bret C. Mobley<sup>7</sup>, Dao-Fu Dai<sup>8</sup>, Vernat Exil<sup>9</sup>, Annet Kirabo<sup>10</sup>, Yan Ru Su<sup>11</sup>, Kelsey Tomasek<sup>11</sup>,  
8 Xiuqi Zhang<sup>11</sup>, Celestine Wanjalla<sup>11</sup>, David L. Hubert<sup>12</sup>, Mark A. Phillips<sup>12</sup>, Melanie R.  
9 McReynolds<sup>3</sup>, Brian Glancy<sup>#2,13</sup>, Antentor Hinton, Jr<sup>#1</sup>

10 **Affiliation:**

11 <sup>1</sup> Department of Molecular Physiology and Biophysics, Vanderbilt University, Nashville, TN.

12 <sup>2</sup> Muscle Energetics Laboratory, NHLBI, NIH, Bethesda, MD, 20892, USA.

13 <sup>3</sup> Department of Biochemistry and Molecular Biology, The Huck Institute of the Life Sciences,  
14 Pennsylvania State University, State College, PA 16801

15 <sup>4</sup> Department of Internal Medicine, University of Iowa, Iowa City, IA, 52242, USA.

16 <sup>5</sup> Department of Medicine, Washington University School of Medicine, St. Louis, MO, USA.

17 <sup>6</sup> UCLA Cardiac Arrhythmia Center, University of California, Los Angeles, CA, USA.

18 <sup>7</sup> Department of Pathology, Vanderbilt University Medical Center, Nashville, TN, 37232 USA.

19 <sup>8</sup> Department of Pathology, Johns Hopkins University School of Medicine, Baltimore, MD, USA

20 <sup>9</sup> Department of Pediatrics, Div. of Cardiology, St. Louis University School of Medicine, St.  
21 Louis, MO, 63104, USA

22 <sup>10</sup> Department of Medicine, Vanderbilt University Medical Center, Nashville, Tennessee, USA.

23 <sup>11</sup> Department of Medicine, Division of Infectious Diseases, Vanderbilt University, Nashville,  
24 TN, 37232, USA.

25 <sup>12</sup> Department of Integrative Biology, Oregon State University, Corvallis, OR, 97331, USA

26 <sup>13</sup> NIAMS, NIH, Bethesda, MD, 20892, USA.

27

28

29

30 \*These authors share co-first authorship.

31 #These authors share senior authorship.

32

33 Corresponding Author:

34 Antentor Hinton

35 Department of Molecular Physiology and Biophysics

36 Vanderbilt University

37 [antentor.o.hinton.jr@Vanderbilt.Edu](mailto:antentor.o.hinton.jr@Vanderbilt.Edu) 319-383-3095

38

39 **Keywords:** Mitochondria, myofibril, heart failure, MICOS complex, 3D reconstruction

40

41 **Abstract:**

42 This study, utilizing SBF-SEM, reveals structural alterations in mitochondria and myofibrils in  
43 human heart failure (HF). Mitochondria in HF show changes in structure, while myofibrils  
44 exhibit increased cross-sectional area and branching. Metabolomic and lipidomic analyses  
45 indicate concomitant dysregulation in key pathways. The findings underscore the need for  
46 personalized treatments considering individualized structural changes in HF.

47 **Letter Text:**

48 Mitochondria are critical in the heart, providing the energy needed for regular heart function;  
49 recent research has identified that mitochondrial dysfunction contributes to heart failure (HF),  
50 and understanding characteristics of mitochondrial dysfunction in failing hearts may assist in  
51 developing new targets for treatment<sup>1</sup>. In experimental models of HF, mitochondria frequently  
52 become swollen and/or fragmented, with disorganized cristae<sup>2</sup>. Alteration in mitochondrial  
53 ultrastructure, may affect the efficiency of ATP production, and may account for mitochondrial  
54 dysfunction in heart failure<sup>2</sup>. This offers a plausible structural-dependent mechanism by which  
55 mitochondrial dysfunction in HF contributes to pathophysiology.

56 To explore this paradigm, we used a previously established method of serial block face-scanning  
57 electron microscopy (SBF-SEM)<sup>3</sup>, to perform 3D reconstruction of mitochondria in similarly  
58 aged human samples with and without HF (Fig. A). The wide x- and y-plane dimensions of SBF-  
59 SEM make it ideal for studying mitochondrial biogenesis, networks, and alterations across  
60 regions of the heart<sup>3</sup>. From the left ventricle, intermyofibrillar mitochondria, which are located  
61 between myofibrils, were manually segmented and analyzed (Fig. A). Mitochondria in HF had  
62 increased volume, surface area, and perimeter, with a tremendous inter-sample variability (Fig.  
63 B). This increased size indicates a greater capacity for ATP generation<sup>3</sup>. Further consideration of  
64 how mitochondrial complexity alters shows that in HF, mitochondria take much more complex  
65 and less spherical phenotypes (Fig. C). Mitochondrial shapes including donut phenotypes and  
66 nanotunnels occur with HF, while the majority of control samples are more spherical, although

67 each patient exhibited unique mitochondrial shapes. Thus, mitochondrial structure demonstrates  
68 tremendous variability, with certain structures that may be characteristic of HF.

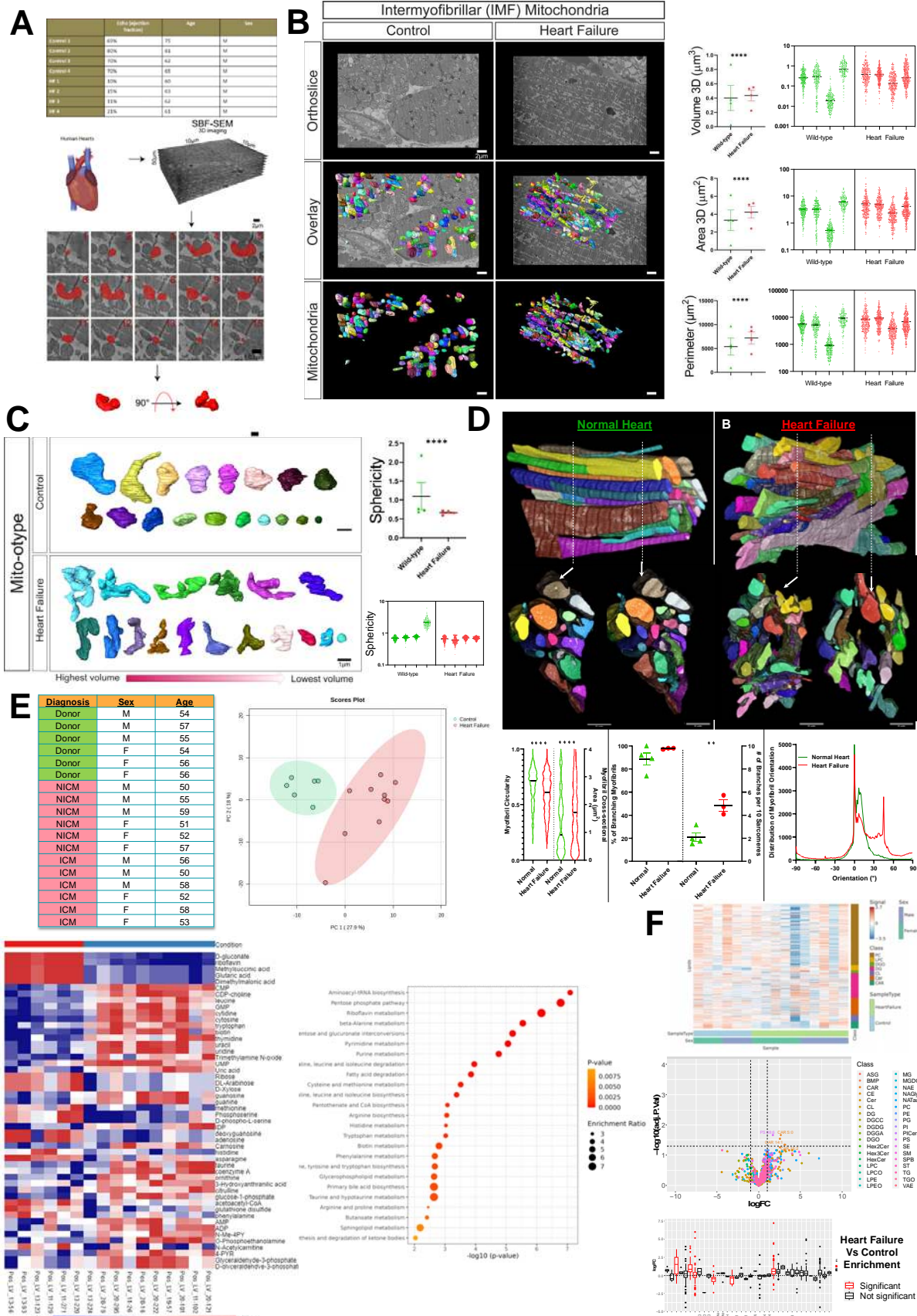
69 From there, the myofibrillar apparatus was considered per previous techniques <sup>4</sup>. The  
70 myofibrillar apparatus is the primary site of ATP utilization in the heart and plays a crucial role in  
71 subcellular remodeling including undergoing significant changes at the structural level during the  
72 development of HF. Myofibrils in HF had a greater cross-sectional area and reduced circularity  
73 per myofibril compared to control myofibrils (Fig. D). The percentage of myofibrils within the  
74 field of view of our datasets with at least one branching sarcomere, as well as the frequency of  
75 branches (Fig. D) was highest during HF as compared with control. Under control conditions, the  
76 myofibrillar apparatus was highly aligned, characterized by a prominent peak at 0° (representing  
77 perfect alignment) and another peak at 8° (Fig. D). However, in the HF condition, a greater  
78 proportion of myofibrils were observed to be oriented at angles of 0°, 7°, and 45°. Thus,  
79 cardiomyocyte sarcomere branching is a pathological feature and reflects parallel remodeling of  
80 the major ATP-producing and utilizing machinery during heart failure.

81 From there, we shifted our attention to how these 3D structural rearrangements concomitantly  
82 occur alongside altered metabolomics and lipidomics. As previously established <sup>3</sup>, principal  
83 component analysis showed tremendous differences in enriched metabolites upon HF (Fig. E).  
84 Heatmaps show increased expression of numerous metabolites in HF, notably, pathway  
85 enrichment shows upregulation of signaling pathways including aminoacyl-tRNA biosynthesis  
86 and pentose phosphate pathway (PPP) (Fig. E). Notably, the PPP plays a critical role in  
87 modulating oxidative stress and glucose oxidation<sup>5</sup>, suggesting dysregulation of it may be  
88 associated with abhorrent mitochondrial function characteristic of HF. Beyond this, riboflavin,  
89 also known as vitamin B2, is a precursor for coenzymes flavin mononucleotide and flavin  
90 adenine dinucleotide, which is important in energy production <sup>6</sup>. Through co-activation of acyl-  
91 CoA, riboflavin may act in a compensatory mechanism, reducing oxidative stress and alliterating  
92 impaired energy production <sup>6</sup>. Lipidomic analysis further shows that although lipid length did not  
93 change, there are differences among individuals with heart failure with upregulation of classes  
94 including acylcarnitines (Fig. F). These have previously arisen as key biomarkers in HF <sup>7</sup>.  
95 Together, this illustrates that mitochondrial and fiber structural alterations concurrently occur  
96 alongside altered enrichment pathways, indicating potential mechanisms to restore pathological  
97 structure.

98 Given that mitochondrial bioenergetics are necessitated in both systolic and diastolic heart  
99 function <sup>1,2</sup>, the mechanisms that govern and alter mitochondria in HF cases remain an intriguing  
100 future avenue. Past research has found that in HF, mitochondria exhibit key signs of dysfunction  
101 including decreased ETC activity, changes in ion activity, and altered dynamics <sup>1,2</sup>. Here, we  
102 have also established that varying subpopulations of mitochondria undergo changes in  
103 nanotunnels and mitochondrial structural arrangement, while the wider spatial orientation of  
104 cardiac myofibrils further changes. Our results highlight the importance of consideration of  
105 mitochondria structure in the treatment of HF, which may vary tremendously between  
106 individuals, both dependent and independent of HF status. Broadening physiological  
107 implications of these unique shapes, and how their relative abundance may be affected by protein  
108 quantity and spatial arrangement may offer insight for personalized medicine. While past studies  
109 have looked at general age-dependent mitochondrial structural changes <sup>3</sup>, equally important is  
110 the consideration of mitochondrial remodeling that occurs in an age-dependent manner after

111 challenges including HF. Other types of HF may further display different mitochondrial  
112 organization, metabolism, and lipid distribution which must be further explicated. Consideration  
113 of how mitochondria and myofibril structure change in dependence on pathophysiology, may  
114 offer an avenue for individualized medicine that targets HF through modulation of mitochondrial  
115 structure.

**116 Figure and Legend**



118 (A) Through existing institutional review board approval (#41148), male human heart failure  
119 (HF) dilated cardiomyopathy samples (ejection fraction between 10-21% and ages between 60-  
120 63) and controls (ejection fraction between 69-80% and ages between 62-81) were collected  
121 (n=4). Serial block face scanning electron microscopy (SBF-SEM) was utilized for manual  
122 contour segmentation of mitochondria from orthoslices. (B) Representative SBF-SEM orthoslice,  
123 3D reconstructions of mitochondria, and isolated mitochondria in control and HF. Mitochondrial  
124 volume, surface area, and perimeter are all displayed, with the averages of each sample shown to  
125 the left, while the right shows dots representing values of each mitochondrion in samples. (C)  
126 Mito-otyping, a method of organizing mitochondria on the basis of their volume, shows the  
127 relative changes in mitochondria structure in HF samples, which are quantified based on  
128 sphericity. (D) Raw SBF-SEM image volumes were rotated in 3D to visualize the muscle cell's  
129 cross-section. Myofibrillar cross-sectional area (CSA) and circularity were measured by  
130 converting the traced structures to binary images and using the Analyze Particles plugin in  
131 ImageJ for each slice throughout the volume (control n=4 humans, 6 cells, 133 myofibrils,  
132 1118 sarcomeres; HF n=3 humans, 12 cells, 219 myofibrils, 2428 sarcomeres). The  
133 distribution data reflects how much of the myofibrillar volume is perfectly aligned (0°) versus  
134 misaligned (away from 0°). (E) Metabolomic analysis comparing Ischemic Cardiomyopathy  
135 (ICM), Non-Ischemic Cardiomyopathy (NICM), and donor samples (n=6) from a mixture of age-  
136 matched males and females. Principal component analysis and metabolic heatmap showing the  
137 relative abundance of metabolites in control and HF. Enrichment analysis and pathway impact  
138 for metabolites enriched in HF. (F) Using the same samples, lipidomic analysis compared HF  
139 and control, showing differences in lipid classes by sex in heatmaps, lipid class (as shown in  
140 volcano plots and box plot), and differences in lipid chain length. For all panels, dot-plots show  
141 mean±SEM, and the numbers of independent samples are indicated, \*\*\*\*,  $p < 0.0001$ ; \*\*,  $p <$   
142 0.001; \*\*,  $p < 0.01$ ; \*,  $p < 0.05$ , calculated with Student's *t*-test.

143

#### 144 **References:**

- 145 1. Brown DA, Perry JB, Allen ME, Sabbah HN, Stauffer BL, Shaikh SR, et al. Mitochondrial  
146 function as a therapeutic target in heart failure. *Nat Rev Cardiol* 2017;14:238–250.  
147 doi:10.1038/nrccardio.2016.203.
- 148 2. Daghistani HM, Rajab BS, Kitmitto A. Three-dimensional electron microscopy techniques for  
149 unravelling mitochondrial dysfunction in heart failure and identification of new  
150 pharmacological targets. *British Journal of Pharmacology* 2019;176:4340–4359.  
151 doi:10.1111/bph.14499.
- 152 3. Vue Z, Garza-Lopez E, Neikirk K, Katti P, Vang L, Beasley H, et al. 3D Reconstruction of  
153 Murine Mitochondria Exhibits Changes in Structure Across Aging Linked to the MICOS  
154 Complex. *Aging Cell* 2023;2022.03.22.485341. doi:10.1101/2022.03.22.485341.
- 155 4. Willingham TB, Kim Y, Lindberg E, Bleck CK, Glancy B. The unified myofibrillar matrix for  
156 force generation in muscle. *Nature Communications* 2020;11:1–10.
- 157 5. Doenst T, Nguyen TD, Abel ED. Cardiac Metabolism in Heart Failure - Implications beyond  
158 ATP production. *Circ Res* 2013;113:709–724. doi:10.1161/CIRCRESAHA.113.300376.
- 159 6. Peng H, Xie M, Zhong X, Su Y, Qin X, Xu Q, et al. Riboflavin ameliorates pathological  
160 cardiac hypertrophy and fibrosis through the activation of short-chain acyl-CoA

161 dehydrogenase. European Journal of Pharmacology 2023;954:175849.  
162 doi:10.1016/j.ejphar.2023.175849.  
163 7. Hunter WG, Kelly JP, McGarrah RW, Khouri MG, Craig D, Haynes C, et al. Metabolomic  
164 Profiling Identifies Novel Circulating Biomarkers of Mitochondrial Dysfunction Differentially  
165 Elevated in Heart Failure With Preserved Versus Reduced Ejection Fraction: Evidence for  
166 Shared Metabolic Impairments in Clinical Heart Failure. Journal of the American Heart  
167 Association n.d.;5:e003190. doi:10.1161/JAHA.115.003190.  
168

## 169 FUNDING

170 This project was funded by the National Institute of Health (NIH) NIDDK T-32, number  
171 DK007563 entitled Multidisciplinary Training in Molecular Endocrinology to Z.V.; National  
172 Institute of Health (NIH) NIDDK T-32, number DK007563 entitled Multidisciplinary Training in  
173 Molecular Endocrinology to A.C.; Integrated Training in Engineering and Diabetes", Grant  
174 Number T32 DK101003; Burroughs Wellcome Fund Postdoctoral Enrichment Program  
175 #1022355 to D.S.; The UNCF/ Bristol-Myers Squibb (UNCF/BMS)- E.E. Just Postgraduate  
176 Fellowship in Life sciences Fellowship and Burroughs Wellcome Fund/ PDEP #1022376 to  
177 H.K.B.; NSF MCB #2011577I to S.A.M.; NSF EES2112556, NSF EES1817282, NSF  
178 MCB1955975, and CZI Science Diversity Leadership grant number 2022-253614 from the Chan  
179 Zuckerberg Initiative DAF, an advised fund of Silicon Valley Community Foundation to S.D.;  
180 The UNCF/Bristol-Myers Squibb E.E. Just Faculty Fund, Career Award at the Scientific  
181 Interface (CASI Award) from Burroughs Wellcome Fund (BWF) ID # 1021868.01, BWF Ad-hoc  
182 Award, NIH Small Research Pilot Subaward to 5R25HL106365-12 from the National Institutes  
183 of Health PRIDE Program, DK020593, Vanderbilt Diabetes and Research Training Center for  
184 DRTC Alzheimer's Disease Pilot & Feasibility Program. CZI Science Diversity Leadership grant  
185 number 2022- 253529 from the Chan Zuckerberg Initiative DAF, an advised fund of Silicon  
186 Valley Community Foundation to A.H.J.; and National Institutes of Health grant HD090061 and  
187 the Department of Veterans Affairs Office of Research award I01 BX005352 (to J.G.). Howard  
188 Hughes Medical Institute Hanna H. Gray Fellows Program Faculty Phase (Grant# GT15655  
189 awarded to M.R.M); and Burroughs Wellcome Fund PDEP Transition to Faculty (Grant#  
190 1022604 awarded to M.R.M). Additional support was provided by the Vanderbilt Institute for  
191 Clinical and Translational Research program supported by the National Center for Research  
192 Resources, Grant UL1 RR024975-01, and the National Center for Advancing Translational  
193 Sciences, Grant 2 UL1 TR000445-06 and the Cell Imaging Shared Resource. Its contents are  
194 solely the responsibility of the authors and do not necessarily represent the official view of the  
195 NIH. The funders had no role in study design, data collection and analysis, decision to publish,  
196 or preparation of the manuscript.

197

## 198 CONFLICT OF INTEREST

199 The authors declare that they have no conflict of interest.

200

## 201 Data Availability

**202** The methods, data, and materials are available upon request.

